PHILOSOPHICAL TRANSACTIONS OF THE ROYAL SOCIETY A MATHEMATICAL, PHYSICAL & ENGINEERING SCIENCES

The Fermi Surfaces of the Noble Metals

M. R. Halse

Phil. Trans. R. Soc. Lond. A 1969 **265**, 507-532
doi: 10.1098/rsta.1969.0064

THE FERMI SURFACES OF THE NOBLE METALS

By M. R. HALSE
Royal Society Mond Laboratory, University of Cambridge

(*Communicated by D. Shoenberg, F.R.S.—Received* 12 *March* 1969)

CONTENTS

Precision measurements of the angular dependence of the de Haas–van Alphen frequencies F (proportional to extremal areas of the Fermi surface) of the noble metals have been made, using the technique of following the oscillations in magnetic properties as the crystal is slowly rotated in a fixed magnetic field. The most thorough measurements were on copper and these and a few measurements on silver agree very well with the results of Joseph, Thorsen, Gertner & Valby (1966) and Joseph & Thorsen (1965); a few measurements were also made on gold to clear up some slight discrepancies between the data of Joseph, Thorsen & Blum (1965) and of Shoenberg (1962).

The major part of the paper is concerned with the use of the most reliable data from all available sources to compute analytical representations of the Fermi surfaces in the form of Fourier expansions. The method of analysis is essentially the same as that used by Roaf (1962) to fit the data of Shoenberg (1962), but because of the greater accuracy and comprehensiveness of the data now available, an appreciably greater accuracy could be achieved in the formulae for the Fermi surfaces. Following Roaf, the volumes of the computed Fermi surfaces were chosen to be exactly those of the free-electron sphere and the excellent agreement between the computed and observed *absolute* values of F, demonstrates the validity of this assumption. The computed orientation dependence of F agreed with experiment not only in regions between fitting points but also as regards features not used in the fitting. In particular, the analytical formulae predicted non-central minima of area whose angular dependence agreed almost exactly with the behaviour of the subsidiary belly oscillations observed by Joseph & Thorsen. Moreover, the existence of a new non-central minimum area (the 'lemon') predicted by the formulae for copper and gold was confirmed experimentally in copper with F in close agreement with the computed prediction. The computed radius vectors of 5 and 7 coefficient formulae for the same metal (with unrelated coefficients) agree to within about 0.2% and this suggests that the formulae are reliable to this sort of accuracy in the radius vector; this compares with the accuracy of order 1% achieved by Roaf.

Once the extremal areas of cross-section of the Fermi surface are known, those of a surface of constant energy slightly differing from the Fermi energy E_F can be immediately deduced if the cyclotron masses

Vol. 265. A. 1167. (Price 14*s*.; U.S. $1.80) 53 [Published 31 December 1969

are known. Using five representative masses, analytical expressions were constructed for surfaces of energy $E_F \pm \Delta E$ and the Fermi velocity v could then be calculated at every point on the Fermi surface. The density of states and hence the electronic specific heat γT could also be deduced; the value of γ computed in this way proved to be in good agreement with experiment. The $\pm$ analytical formulae are also useful in providing a reliable interpolation and extrapolation between the cyclotron mass data used in fitting the formulae. From the cyclotron masses at the points where de Haas–van Alphen amplitude vanishes, values of the spin-splitting factor g for copper were deduced which differ appreciably from direct spin resonance measurements. Finally, the computed orientation dependence of surface resistance in the anomalous skin effect is shown to agree fairly well with experiment, though at a few points, particularly in silver, there are discrepancies which may be significant.

Introduction

Some years ago, on the basis of Shoenberg's (1962) de Haas–van Alphen effect data, Roaf (1962) expressed the Fermi surfaces† of the noble metals (Cu, Ag, Au) analytically in the form of Fourier expansions, with an accuracy of order 1 % in radius vector. Recent developments in the measurement of the de Haas–van Alphen effect have brought considerable improvements and in particular the technique of observing oscillations as the sample is rotated in a fixed field, allows differences of Fermi surface cross-sectional area with orientation to be measured about five or ten times more accurately than before, and with a more continuous coverage of orientation.

The present investigation was started with the intention of exploiting this technique to obtain appreciably better expressions for the Fermi surfaces. Such greater accuracy is potentially of value in enabling more crucial comparisons to be made with theory and also in providing more reliable estimates of differential properties of the Fermi surfaces such as are required for comparison with various other kinds of experiment.

Soon after the present experiments had started, it was learned that similar experiments on silver and gold (but using the torque method rather than field modulation) had been completed in California (Joseph & Thorsen 1965; Joseph, Thorsen & Blum 1965), and that measurements on copper were in progress. In spite of this it was thought worth while to continue the experiments in order to have an independent check by a somewhat different method, but it was decided to put the main emphasis on copper, for which no new results had yet appeared. In the event, the present measurements on copper proved to agree very well with those of the California group (Joseph, Thorsen, Gertner & Valby 1966), as did the preliminary measurements on silver, although these were much less complete. A few measurements were also made on gold to resolve some slight but significant discrepancies between the data of various authors.

The major part of this paper is concerned with the analysis of the de Haas–van Alphen data to obtain analytical expressions for the Fermi surfaces of the three metals and the derivation of various properties which required a knowledge of the Fermi surfaces. A series of 'best' values for certain parameters of the experimental data were chosen on the basis of a critical comparison of the California results, the present results and older ones, and these were used to determine the coefficients of Roaf type formulae for the Fermi surface. The radius vectors of these new surfaces are probably reliable to something like 0.2 %.

The computing program was such that non-central as well as central, cross-sectional areas of a given surface could be determined and computation revealed that for certain directions the belly area as a function of perpendicular distance from the centre of the surface showed a minimum away from the centre. These non-central minimum areas proved to be in excellent agreement with

† The general appearance of the Fermi surface and the nomenclature for various extremal orbits (e.g. belly, neck, dog's bone, etc.) are described in Shoenberg (1962).

PHILOSOPHICAL TRANSACTIONS OF THE ROYAL SOCIETY A MATHEMATICAL, PHYSICAL & ENGINEERING SCIENCES

the areas corresponding to subsidiary belly frequencies observed by both the California group and in the present work, and which Joseph & Thorsen had in fact provisionally attributed to just such non-central extremal areas. This agreement of computed and observed values for the non-central extremal areas is all the more striking since no use was made of the experimental data on these areas in deriving the formulae for the Fermi surface. It was also computed that there should be a non-central extremum, shaped like a lemon, normal to ⟨110⟩, and evidence for this has been found by a special experiment, again in excellent quantitative agreement with the computed prediction.

Once the Fermi surface is known, a detailed knowledge of cyclotron mass as a function of orientation should permit computation of the immediately neighbouring surfaces of constant energy, and hence the derivation of the Fermi velocity as a function of position on the Fermi surface and also of the density of states at the Fermi surface. Roaf had attempted to carry through such calculations, but was unsuccessful because the cyclotron mass data then available were not accurate enough. In the meantime new and more accurate cyclotron mass data have become available and these have been used in conjunction with the more accurate expressions for the Fermi surface to complete this program; this is the first time the Fermi velocity has been determined in this way. The densities of states proved to be in excellent agreement with the values deduced from the electronic specific heats. A by-product of the computations is in providing an interpolation between the observed cyclotron masses and also in predicting the cyclotron mass of orbits which have not been observed in cyclotron resonance, e.g. the lemon-shaped orbit, the 6-cornered rosette and non-extremal orbits. The cyclotron masses at orientations where the de Haas–van Alphen amplitude vanishes have been used to deduce g values for the extremal orbits at these orientations.

Finally the anomalous skin effect for copper and silver was computed from the new Fermi surface formulae and found to be reasonably consistent with the experimental data. The agreement is however little better than that achieved originally by Roaf with Cu IV and Ag IV and the present analysis suggests that his six term surfaces Cu VI and Ag VI, constructed to improve the fit to anomalous skin effect, now depart too far from the de Haas–van Alphen effect data. In addition, some of the published properties of Cu VI are believed to contain computational errors.

Experimental details

The main measurements were of de Haas–van Alphen oscillations as a function of angle of rotation in the fixed field (usually about 5 T (50 kG)) of a superconducting magnet in the persistent mode, although a few additional measurements were also made in which the orientation was fixed and the field varied. From the angular variation at fixed field H it is easy to deduce changes of the de Haas–van Alphen frequency† F with orientation since each complete oscillation corresponds to $\Delta F/H = 1$. The variation with field at fixed orientation was used to make comparisons between frequencies of different features (e.g. belly and neck).

Details of the field modulation technique (Shoenberg & Stiles 1964) used for detecting the oscillations have been amply described in the literature (see, for example, Windmiller & Ketterson 1968), and so only the novel points of the present work need be mentioned. The main

† This frequency F is proportional to the extremal area A of the Fermi surface. Since we shall mostly be concerned with *ratios* of frequencies which are identical with area ratios, the terms frequency and area will often be used interchangably.

PHILOSOPHICAL TRANSACTIONS OF THE ROYAL SOCIETY A MATHEMATICAL, PHYSICAL & ENGINEERING SCIENCES

innovation was the use of fixed pick-up and modulation coils symmetrically disposed about the specimen (thus avoiding noise associated with moving coils), and the use of a special method (Pippard & Sadler 1969) for smooth rotation of the specimen about a horizontal axis. The device was very carefully calibrated so that the orientation of the specimen was known to about 0.2° at all stages of its rotation; such accuracy is essential if full advantage is to be taken of the improved precision of the frequency determination.

Care was taken to keep the desired crystallographic zone axis of the specimens perpendicular to the magnetic field to within 1°. Experiments were performed on three silver, three gold, and seven copper crystals in the {100} and {110} zones and on three copper crystals in the {211} zone. The copper crystals which were of high purity and mechanical quality (resistance ratio of a few thousands) were obtained from Dr I. M. Templeton of N.R.C., Ottawa; the silver and gold crystals were cut out of crystal ingots of only moderate purity (resistance ratio of the order of 10^2).

Experimental results

Copper

Part of an experimental rotation curve (in the {110} zone from $\theta = 0$ to 26°) is reproduced in figure 1 and illustrates features typical of all three metals and of other angular ranges. Around $\theta = 0°$ (i.e. ⟨100⟩) the faster oscillations are due to the rosette whose area varies more rapidly with angle than the area of the central belly which is responsible for the main oscillations. At about $\theta = 16.0°$ it can be seen that the central belly area goes through a stationary value (a minimum, described as the 'dip' D_1 in Shoenberg's notation), and then increases more and more rapidly. The faster superimposed oscillations are from the non-central belly extremum and with increasing θ the difference between the central belly frequency (F_{B1}) and the non-central one (F_{B2}) decreases. At $\theta = 23.0 \pm 0.1°$, $F_{B1} - F_{B2}$ vanishes and the amplitude of the oscillations blows up in the 'merging' region because of the large value of the curvature factor $(\partial^2 A/\partial k_z^2)^{-\frac{1}{2}}$. Beyond $\theta = 25.5°$ the belly oscillations cease owing to the intervention of the necks. At $\theta = 23.7°$ the amplitude becomes small because of a vanishing spin-splitting factor for the central belly; there is also a vanishing spin-splitting factor at $\theta \simeq 22°$ for the non-central belly (a detailed discussion of spin-splitting zeros will be given later (see p. 529)).

From rotation curves of this kind taken in the {100}, {110} and {211} zones, the angular variations of the frequencies F_{B1}, F_{B2}, F_D (dog's bone), F_R (4-rosette) and F_N (neck) were deduced and the results are summarized in table 2 and figures 2 and 3 in which the results of Joseph *et al.* (1966) and values computed from the analytical surface Cu7 (see p. 519) are also shown. All frequency differences are quoted as fractions of the free-electron de Haas–van Alphen frequency F_s (whose values are given in table 1) and hence also represent fractional changes in Fermi surface cross-sectional area. Except for the {211} zone, the r.m.s. error in F/F_s as revealed by the consistency of different runs is typically 5×10^{-4}. The agreement with Joseph *et al.* is on the whole very good, the r.m.s. deviation in the F/F_s values between the present data and theirs being

Figure 1. Experimental rotation curve at 4.9 T (49 kG) for a copper crystal in the {110} zone from $\theta = 0$ to 26°. At this field one oscillation corresponds to $\Delta F/F_s \simeq 8 \times 10^{-5}$. The marked features are: A, 4-rosette and central belly oscillations near ⟨100⟩; B, central belly area at stationary value (the dip D_1) and faster superimposed oscillations due to the non-central belly; C, non-central belly amplitude passes through zero due to a vanishing spin-splitting factor; D, large amplitude at the merging point of the central and non-central belly oscillations; E, belly amplitude passes through zero due to a vanishing spin-splitting factor; F, belly oscillations cease owing to the intervention of the necks; G, pen recorder sensitivity doubled.

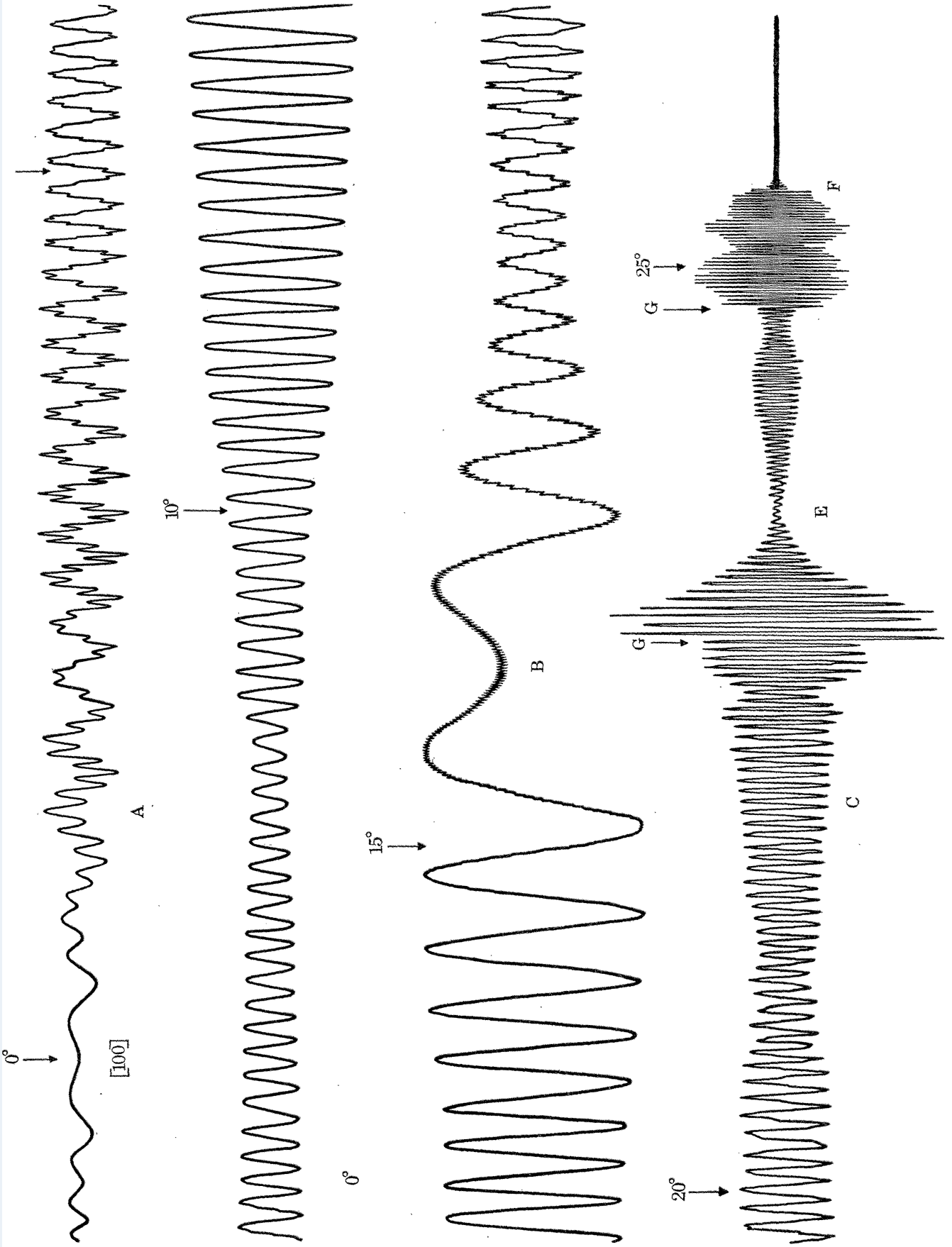

FIGURE 1. For legend see facing page.

PHILOSOPHICAL TRANSACTIONS OF THE ROYAL SOCIETY A MATHEMATICAL, PHYSICAL & ENGINEERING SCIENCES

7×10^{-4}, which is of the same order as the combined uncertainties of the two sets. There was also very good agreement with Joseph *et al.* as regards the angular ranges over which various features could be detected and the merging point angles of central and non-central belly orbits. These various angles are indicated in the notes to table 2.

TABLE 1. VALUES OF LATTICE CONSTANT a AND F_s

metal	$10^8 a$/cm (at 0 K)	$10^{-4} F_s$/T†
Cu	3.6030 ± 4	6.1140 ± 10
Ag	4.0692 ± 8	4.7930 ± 15
Au	4.0652 ± 4	4.8025 ± 10

† 1T = 10^4G.

Notes: F_s is calculated from the formula $F_s = \dfrac{\pi hc}{a^2 e}\left(\dfrac{3}{2\pi}\right)^{\frac{2}{3}}$;

the values of a were taken from the same data as those used by Shoenberg (1962), but the corrections for thermal contraction were calculated more accurately; slight differences between the present estimates of F_s and those of Shoenberg are however mainly due to the use of slightly revised values of the fundamental constants.

The reproducibility of the F variation in the {211} zone between different experiments was appreciably worse, particularly in the region $\psi \gtrsim 50°$, where the r.m.s. error was as much as 30×10^{-4}. This is due to the absence of a mirror plane perpendicular to the {211} zone axis, which makes F extremely sensitive to zone misalinement. Errors of order 1° are sufficient to account for the observed variations in F between experiments, and for the uncertainty of order $\pm 5°$ in the angle, $\psi \simeq 61°$, at which the belly oscillation ceased.

The experiments in which oscillations were recorded as a function of field at fixed orientation permitted accurate determination of the ratios belly: neck and belly: 4-rosette, and gave

$$F_{B111}/F_N = 26.73 \pm 0.02, \quad F_{B100}/F_R = 2.436 \pm 0.002.$$

As can be seen from table 5*a*, these values, which are used as fitting parameters, agree very well with those of Joseph *et al.* (1966). A field variation at $\theta = 18.25°$ produced the expected beats between the central and non-central belly frequencies and the beat frequency agreed within experimental accuracy with the estimate of $F_{B1} - F_{B2}$ deduced from the rotation curves. No superimposed oscillation of this low difference frequency, of the kind observed by Joseph & Thorsen (1965) was found in the field variation of the present experiments. As discussed by Shoenberg (1968), their observation was probably a specific feature of the torque method of measurement used by them.

Silver

The experimental results were far less comprehensive than those of Joseph & Thorsen (1965), but as can be seen from table 3 and figure 4 the agreement is very good where comparison is possible. Since the analysis will be based mainly on Joseph & Thorsen's data, present results will not be described beyond this brief mention, except for a few details which will be quoted later (p. 515).

Gold

In view of the detailed results of Joseph *et al.* (1965) (see table 4) no comprehensive study of the angular variation of F was attempted, but a few experiments were made to clear up some appreciable discrepancies between their data and those of Shoenberg (1962). These were as regards the dip D_1 in the {110} zone and the ratios F_{B100}/F_{B111} and F_{B111}/F_N. As for copper, the

TABLE 2. ORIENTATION DEPENDENCE OF $10^4\Delta F/F_s$ IN COPPER

θ/deg	B_1			R		
0	0	(0)	*0*	0	(0)	
2	−2	(−3)	*−2*	11	(11)	
4	−9	(−10)	*−10*	45	(45)	
6	−19	(−20)	*−20*	107	(106)	
8	−31	(−32)	*−32*	220	(211)	
10	−43	(−44)	*−44*			
12	−53	(−55)	*−55*			
14	−61	(−63)	*−62*		B_2	
16	−64	(−67)	*−65*	−255	(−266)	−268
18	−61	(−64)	*−62*	−157	(−158)	*−163*
20	−52	(−54)	*−51*	−86	(−86)	*−88*
22	−31	(−33)	*−31*	−35	(−37)	*−36*
23	−15	(−18)	*−15*	−15	(−18)	*−15*
24	5	(1)	*4*			
					N	
30				233	(234)	*235*
32				168	(171)	*168*
34				125	(127)	*124*
36				93	(95)	*92*
38				69	(70)	*68*
40				50	(51)	*49*
42				36	(36)	*35*
44				25	(25)	*24*
46	143	(149)	*144*	16	(16)	*15*
48	81	(83)	*80*	9	(9)	*8*
50	39	(40)	*38*	5	(5)	*4*
52	13	(13)	*12*	2	(2)	*2*
54.7	0	(0)	*0*	0	(0)	*0*
56	3	(3)	*3*	0	(0)	*0*
58	17	(17)	*17*	2	(2)	*2*
60	44	(46)	*45*	5	(6)	*5*
62	83	(87)	*86*	10	(11)	*10*
64	137	(141)	*140*	17	(18)	*17*
66	203	(208)	*208*	26	(27)	*26*
68	283	(289)	*290*	38	(38)	*38*
70	386	(386)	*389*	53	(53)	*53*
72	506	(507)	*512*	73	(71)	*72*
74		D		98	(95)	*97*
76	338		*348*	129	(126)	*129*
78	239		*243*	171	(170)	*174*
80	162	(164)	*163*	233	(231)	*238*
82	102	(102)	*101*	324	(330)	*339*
84	57	(56)	*56*			
86	25	(25)	*25*			
88	6	(6)	*6*			
90	0	(0)	*0*			

ϕ/deg	B_1			R		
0	0	(0)	*0*	0	(0)	
2	−2	(−2)	*−2*	11	(11)	
4	−9	(−8)	*−9*	46	(44)	
6	−17	(−17)	*−18*	105	(102)	
8	−25	(−25)	*−26*	191	(189)	
10	−32	(−32)	*−32*	318	(318)	
12	−34	(−33)	*−34*			
14	−31	(−29)	*−30*			
16	−22	(−18)	*−19*			
18	−4	(2)	*0*		B_2	
20	23	(30)	*28*	−233	(−229)	*−245*
22	58	(68)	*66*	−117	(−106)	*−122*
24	104	(117)	*114*	−4	(11)	*−1*
26	162	(177)	*174*	106	(125)	*117*
28	234	(250)	*248*	215	(234)	*230*
30	326	(337)	*338*	325	(337)	*338*
32	448	(454)	*456*		D	
34					(467)	*448*
36					(283)	*272*
38				151	(163)	*156*
40				76	(82)	*77*
42				27	(29)	*27*
45				0	(0)	*0*

ψ/deg		
0	0	*0*
2	6	*7*
4	26	*27*
6	60	*61*
8	110	*110*
10	177	*180*
		B_2
34	0	*0*
36	−33	*−39*
38	−63	*−79*
40	−88	*−98*
42	−111	*−127*
44	−134	*−157*
46	−155	*−186*
48	−176	*−212*
50	−193	*−234*
52	−205	*−249*
54	−211	*−258*
56	−210	*−257*
58	−201	*−245*
60	−180	

	B_2
	−3
	−56
	−102
	−136
	−163
	−181
	−193
	−201
	−207
	−211
	−211

Notes. The three entries for $10^4\Delta F/F_s$ in each column refer to the present experimental results, those of Joseph *et al.* (1966) in parentheses and those computed from Cu7 in italics; the angular variations for the non-central belly in the {211} zone and for the rosette were not computed. The angles θ, ϕ, and ψ are from ⟨100⟩ in the {110} and {100} zones and from ⟨111⟩ in the {211} zone respectively. Frequency differences in the {211} zone around $\psi \sim 50°$ have been arbitrarily reckoned from $\psi = 34°$. Merging points of F_{B1} and F_{B2} occurred at $\theta = 23.0 \pm 0.1°$, $\phi = 30.4 \pm 0.2°$, $\psi \sim 33°$ and $\psi \sim 55°$. Observed angular limits of the various orbits were F_R, $\theta = 8.7°$ (8.8°), $\phi = 11.0°$ (10.7°); F_{B1}, $\theta = 25.5°$ (25.58°), $\phi = 44.7°$ (45°), $\theta = 72.9°$ (72.3°), $\phi = 32.4°$ (32.5°), $\psi = 11.3°$; F_{B2}, $\theta = 15°$ (15°), $\phi = 20°$ (19°); F_D, $\theta = 74.2°$ (79.8°), $\phi = 36.3°$ (33.8°); F_N, $\theta = 29.6°$ (28.9°), $\theta = 82.1°$ (83°); the figures in parentheses refer to Joseph *et al.* The angular limits were not computed precisely but are quite consistent with the observed values.

PHILOSOPHICAL TRANSACTIONS OF THE ROYAL SOCIETY A MATHEMATICAL, PHYSICAL & ENGINEERING SCIENCES

dip D_1 was measured in rotation experiments at fixed field. For gold the value of D_1 is more sensitive to slight zone alinement errors than for copper and silver; in fact the values found ranged from 0.0257 to 0.0308. The correct value must be towards the upper end of this range since D_1

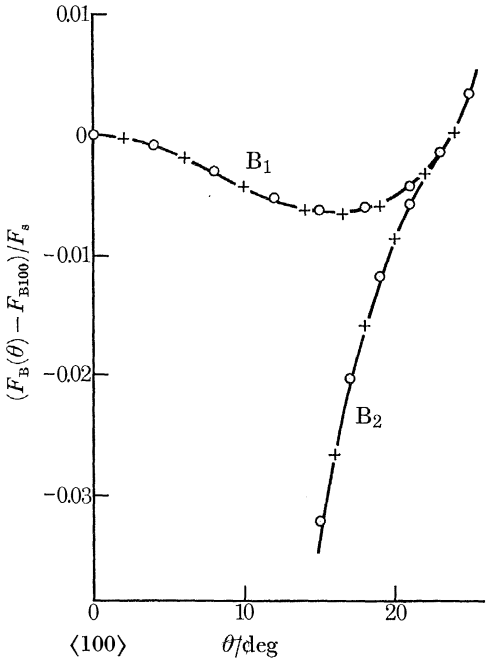

FIGURE 2. Angular variation of F_{B1} and F_{B2} for copper near ⟨100⟩ in a {110} zone; ○, present experiment; +, Joseph *et al.* (1966); ——, computed from Cu7.

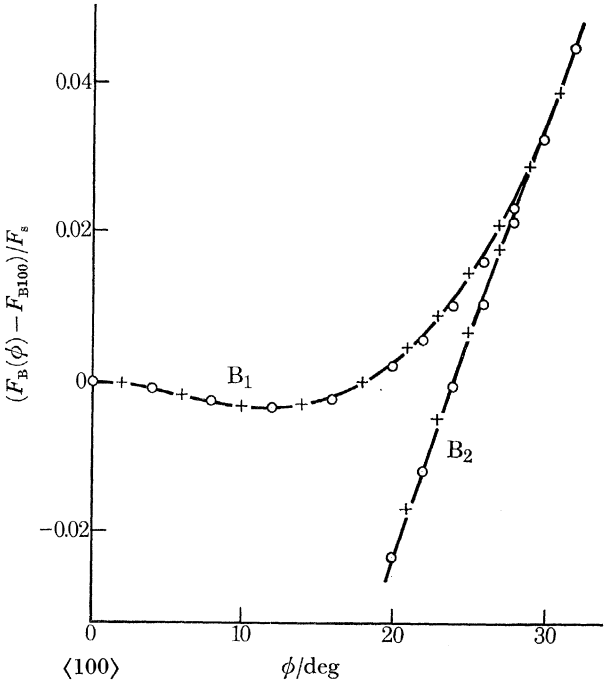

FIGURE 3. Angular variation of F_{B1} and F_{B2} for copper near ⟨100⟩ in a {100} zone; ○, present experiment; +, Joseph *et al.* (1966); ——, computed from Cu7.

is an absolute maximum with respect to angular errors (see Roaf 1962, figure 1) and detailed examination suggests that $D_1 = 0.0306 \pm 0.0010$ (cf. Shoenberg 0.0309, Joseph *et al.* 0.0274) and that the minimum occurs at $\theta = 22.0 \pm 0.4°$ (in fair agreement with both sets of earlier data). In the course of these experiments oscillations from the non-central belly were recorded between $\theta = 21$ and 25° but were not studied in detail.

TABLE 3. ORIENTATION DEPENDENCE OF $10^4 \Delta F/F_s$ IN SILVER

θ/deg	B_1			R		N		ϕ/deg	B_1			B_2	
0	0	(0)	*0*	(0)			*321*	0	0	(0)	*0*	(12)	*7*
2	−2	(−2)	*−2*	(12)		(176)	*176*	2	−2	(−2)	*−2*	(125)	*121*
4	−8	(−8)	*−8*	(54)		(117)	*118*	4	−8	(−7)	*−8*	(231)	*230*
6	−16	(−17)	*−17*	(132)		(83)	*83*	6	−16	(−15)	*−16*	(336)	*332*
8	−26	(−28)	*−28*			(60)	*60*	8	−24	(−23)	*−25*		*D*
10	−37	(−40)	*−40*			(44)	*44*	10	−32	(−31)	*−33*	(188)	*185*
12	−48	(−51)	*−52*			(32)	*32*	12	−37	(−35)	*−39*	(89)	*88*
14	−57	(−61)	*−62*			(22)	*22*	14	−38	(−38)	*−40*	(30)	*30*
16	−65	(−68)	*−69*			(15)	*15*	16	−34	(−34)	*−37*	(4)	*3*
18.1	−70	(−71)	*−72*			(10)	*10*	18	−24	(−25)	*−27*	(0)	*0*
20	−68	(−69)	*−70*	B_2		(6)	*6*	20	−8	(−9)	*−10*		
22	−62	(−62)	*−63*	(−137)	*−137*	(3)	*3*	22	2	(16)	*14*		
24	−48	(−47)	*−48*	(−71)	*−75*	(1)	*1*	24		(46)	*46*		
26	−24	(−25)	*−25*	(−26)	*−28*	(0)	*0*	26		(86)	*85*		
28		(18)	*14*			(0)	*0*	28		(134)	*133*		
30						(2)	*1*	30		(191)	*190*		
32						(4)	*4*	32		(256)	*256*		
34						(7)	*7*	34		(335)	*334*		
36						(11)	*11*	36		(446)	*435*		
38						(17)	*17*	38					
40						(24)	*25*	40					
42						(34)	*34*	42					
44		(153)	*144*	(153)	*144*	(47)	*47*	44					
46		(97)	*94*	(91)		(65)	*65*	45					
48	64	(55)	*56*	(34)		(89)	*90*						
50	34	(28)	*28*	(−17)	*−18*	(125)	*126*	ψ/deg					
52	13	(10)	*10*	(−62)		(187)	*187*	0			*0*		
54.7	0	(0)	*0*	(−116)	*−121*		*316*	2			*5*		
56	2	(2)	*3*	(−102)				4			*20*		
58	14	(12)	*13*	(−74)	*−78*			6			*34*		
60	38	(33)	*34*	(−36)	*−40*			8			*78*		
62	67	(63)	*64*	(10)	*5*			10			*121*		
64	104	(102)	*103*	(62)				12			*176*		
66		(150)	*151*	(121)				14			*248*		
68		(206)	*208*	(188)	*185*								
70		(272)	*274*	(263)				32			*20*		
72		(348)	*348*	(344)				36			*−17*		
74		(433)	*431*	(433)	*428*			40			*−54*		
76		(529)	*524*	*D*				44			*−95*		
78					*302*			48			*−136*		
80				(187)	*190*			50			*−154*		
82				(115)	*115*			52			*−168*		
84				(63)	*63*			54			*−178*		
86				(29)	*27*			56			*−183*		
88				(8)	*7*			58			*−181*		
90				(0)	*0*			60			*−172*		
								62			*−156*		
								64			*−132*		
								66			*−100*		
								68			*−57*		

Notes. The same notation is used as in table 2. The entries in each column refer where applicable to the present experimental results, those of Joseph & Thorsen (1965) in parentheses, and those computed from Ag7 in italics.

TABLE 4. ORIENTATION DEPENDENCE OF $10^4\Delta F/F_s$ IN GOLD

θ/deg	B_1			B_2		ϕ/deg	B_1		B_2	
0	0	(0)	*0*			0	(0)	*0*		
2	−7	(−3)	*−5*			2	(−9)	*−8*		
4	−30	(−16)	*−29*			4	(−31)	*−30*		
6	−63	(−47)	*−65*			6	(−61)	*−59*		
8	−103	(−86)	*−108*			8	(−92)	*−90*		
10	−142	(−126)	*−149*			10	(−120)	*−118*		
12	−183	(−167)	*−192*			12	(−142)	*−141*		
14	−221	(−203)	*−233*			14	(−158)	*−155*		
16	−255	(−234)	*−266*			16	(−164)	*−161*		
18	−281	(−256)	*−292*		(−347) *−382*	18	(−159)	*−155*		
20	−299	(−269)	*−309*		(−299) *−336*	20	(−144)	*−139*		
22	−306	(−273)	*−314*	−320	(−277) *−316*	22	(−119)	*−111*		
24	−298	(−263)	*−306*			24	(−83)	*−71*		
26	−269		*−264*			26	(−33)	*−18*		
						28	(31)	*49*	(−16)	*−9*
						30	(111)	*132*	(101)	*117*
						32	(214)	*238*		
							D			
						36	(294)	*290*		
						38	(168)	*165*		
						40	(82)	*81*		
						42	(29)	*28*		
						44	(4)	*3*		
						45	(0)	*0*		

Notes. The same notation is used as in table 2. The entries in each column refer where applicable to the present experimental results, those of Joseph *et al.* (1965) in parentheses and those computed from Au5 in italics. The frequency variation of features other than those shown here have not been computed systematically; experimental values for F_{B1} over a wider range of θ and for F_R and F_N may be found in Joseph *et al.* (1965). The {110} zone minimum (i.e. D_1) and the merging point of F_{B1} and F_{B2} occurred at $\theta = 22.0°$ and $\theta \simeq 24.4°$ respectively.

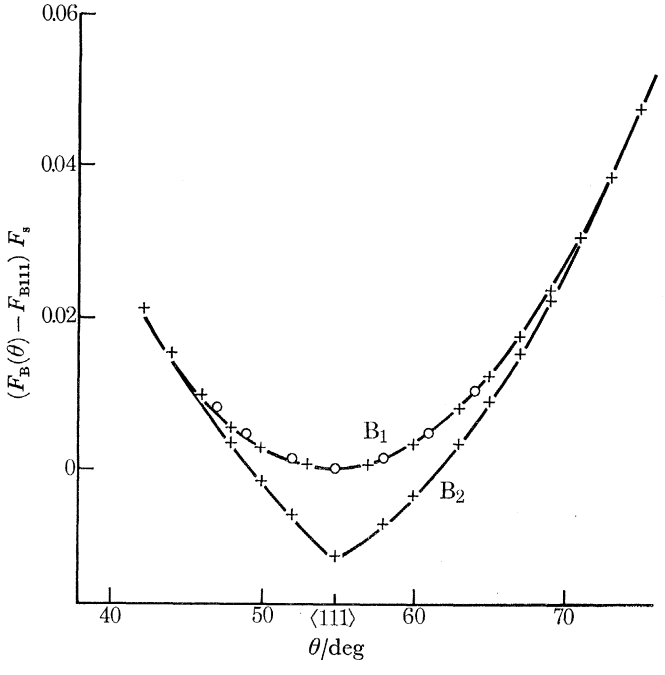

FIGURE 4. Angular variation of F_{B1} and F_{B2} for silver around ⟨111⟩ in a {110} zone; ○, present experiment; +, Joseph & Thorsen (1965); ——, computed from Ag7.

From careful field variation experiments on the same ⟨110⟩ crystal in the same helium experiment (thus eliminating magnet calibration errors) the ratio F_{B100}/F_{B111} was found to be 1.0765 ± 0.0015 (cf. Shoenberg 1.077, Joseph *et al.* 1.099). Assuming $F_{B100}/F_s = 1.009$ (from Shoenberg's result which is accurate enough for the purpose) we deduce that

$$D \equiv (F_{B100} - F_{B111})/F_s = 0.0717 \pm 0.0015$$

(cf. Shoenberg 0.0722). The field variation at ⟨111⟩ also gave $F_{B111}/F_N = 29.26 \pm 0.05$ (cf. Shoenberg 29.93, Joseph *et al.* 29.27). Since these measurements were made a more accurate determination by Jan & Templeton (1967) has given this ratio as 29.33 ± 0.03 and this value was used as the fitting parameter for Au5.

Derivation of the Fermi surfaces

Analytical representation

Following Roaf, the choice of analytical representation of the Fermi surfaces was in the form of a Fourier series:

$$\begin{aligned} C_0 = {} & 3 - \Sigma \cos \tfrac{1}{2}ak_y \cos \tfrac{1}{2}ak_z + C_{200}(3 - \Sigma \cos ak_x) \\ & + C_{211}(3 - \Sigma \cos ak_x \cos \tfrac{1}{2}ak_y \cos \tfrac{1}{2}ak_z) + C_{220}(3 - \Sigma \cos ak_y \cos ak_z) \\ & + C_{310}(6 - \Sigma \cos \tfrac{3}{2}ak_x \cos \tfrac{1}{2}ak_y - \Sigma \cos \tfrac{3}{2}ak_y \cos \tfrac{1}{2}ak_x) + C_{222}(1 - \cos ak_x \cos ak_y \cos ak_z) \\ & + C_{321}(6 - \Sigma \cos \tfrac{3}{2}ak_x \cos ak_y \cos \tfrac{1}{2}ak_z - \Sigma \cos \tfrac{3}{2}ak_z \cos ak_y \cos \tfrac{1}{2}ak_x), \end{aligned} \tag{1}$$

where the summation signs indicate commutation of x, y, and z, a is the lattice constant (see table 1), k_x, k_y, k_z, are the coordinates in k space of a point on the surface and the C are coefficients to be fitted to the experimental area data. A feature of this expansion which might conceivably cause difficulty when dealing with open orbits is the existence of multiple solutions for certain directions of k. These solutions appear as unwanted sheets of surface devoid of physical significance and must be ignored. The computing procedure used was such that once the correct surface had been located all orbits could be traversed without leaving that surface by more than a prescribed amount; this procedure will not be described since it is essentially similar to that used by Roaf.

The choice of the number of coefficients used for the representation of each Fermi surface was dictated by a balance between complexity of computation, which increased rapidly with the number of terms and the need to fit as many experimental features as possible. Both five and seven coefficient expansions were investigated and the good agreement found between them in spite of the fact that the coefficients in the two were totally unrelated, suggests that not much would be gained by going to a greater number of coefficients.

Fitting parameters and surface construction

The method of constructing a surface also closely follows Roaf. Thus to fit seven experimental features,† say x_i, an initial guess is made at the values of the seven coefficients C_j which appear in equation (1) (the values of one of Roaf's surfaces might, for instance, be chosen) and the values of the relevant features are computed. In general these values will be somewhat different from

† Strictly speaking only six of these, the areas at certain orientations, are experimental; the seventh is the volume, which is taken to be exactly that of the free-electron sphere.

those it is desired to fit and a systematic procedure is followed to modify the initial coefficients appropriately. By varying one coefficient at a time by a given small amount the relevant properties of seven related surfaces are found, enabling the 49 coefficients $\partial x_i/\partial C_j$ for the trial surface to be determined. A first approximation to the required modification of the C (assuming the x_i vary linearly with the C_j) then follows from the solution of seven simultaneous equations. However, since the problem is not sufficiently linear, the first such approximation may be quite inadequate and new derivatives $\partial x_i/\partial C_j$ have to be computed for the new surface produced by such an extrapolation. Typically, ten such successive approximations were needed before the computed values of the x fell within experimental error of the values to be fitted. Use was also made of the fact that the properties of a surface with coefficients $\frac{1}{2}(C_j + C'_j)$ are approximately the arithmetic means of the properties of the two surfaces defined by C_j and C'_j.

In all the surfaces one of the features chosen for fitting was the volume of the surface which was made exactly equal to the free electron volume (i.e. $V/V_s = 1$). Only differences of nearly equal frequencies and frequency ratios were used as the other fitting features, so that calibration errors of absolute frequencies were either only slightly involved (in the differences) or not at all (in the ratios). As we shall see later (p. 520) the absolute values of F/F_s computed from the final analytical surfaces are in excellent agreement with the most reliable absolute experimental values and this agreement shows that the assumption $V/V_s = 1$ is justified. Considerable computing accuracy was required to avoid introducing computing errors comparable with the experimental errors and the accuracy achieved was such that the computing errors in F/F_s, in small differences $\Delta F/F_s$ and in V/V_s did not exceed 10^{-4}, 2×10^{-5}, and 5×10^{-4} respectively. In the calculation of the density of states (see p. 528) this accuracy of computing V/V_s was not quite adequate and special steps were taken to reduce the computing error in V/V_s to 2×10^{-4}.

The details of the parameters used in computing the copper, silver and gold surfaces are summarized in table 5, together with the estimates of these parameters by various authors and the values characteristic of the various computed surfaces. The values of the coefficients of the various computed surfaces are collected in table 6. As well as the fitting parameter $V/V_s = 1$ all the surfaces have in common the use of the ratio F_{B111}/F_N, of $D = (F_{B100} - F_{B111})/F_s$, and the dips D_1 and D_2 in the {110} and {100} zones.

Properties of the computed surfaces

The finally computed surfaces are intended to be accurate representations of the Fermi surfaces and their properties will now be examined and compared with experiment and with band structure calculations. The most significant comparisons are with de Haas–van Alphen frequencies in regions remote from those used in the fitting procedure and as regards entirely different properties based on the Fermi surface. In the latter category are the anomalous skin effect and also properties such as Fermi velocity and density of states, which, however, require the introduction of cyclotron mass data as well as a knowledge of the Fermi surface.

Absolute frequencies

The values of F/F_s at symmetry directions computed from the new surfaces are given in table 7, where they are compared with available experimental data. The predicted ⟨111⟩ and ⟨100⟩ belly areas are in excellent agreement with experiment (average error 0.1 %) and as already mentioned this confirms the validity of the assumption that $V/V_s = 1$. The accuracy of other

TABLE 5. DATA USED IN FITTING THE FERMI SURFACES

fitting parameter	Shoenberg 1962	California group	present expt	chosen value	present work computed		Roaf 1962 recomputed	
(*a*) copper					Cu5	Cu7	Cu IV	Cu VI
V/V_s	—	—	—	1.000	1.000	1.000	0.998	0.990*
D	0.0305	—	—	0.0305	0.0306	0.0306	0.0306	0.0311
D_1	0.0062	0.0067	0.00645	0.0066	0.0066	0.0065	0.0061	0.0062
D_2	0.0035	0.00334	0.00342	0.00338	0.00335	0.00341	0.0030	0.0026*
F_{B111}/F_N	—	26.73	26.73	26.73	26.72	26.72	—	23.37
F_{B100}/F_R	—	2.438	2.436	2.437	2.438	2.437	—	2.324
D_3	—	0.0212	0.0196	0.0204	0.0213	0.0209	—	0.0274
(*b*) silver					Ag5	Ag7	Ag IV	Ag VI
V/V_s	—	—	—	1.000	1.000	1.000	1.001	1.002
D	0.0286	—	—	0.0286	0.0285	0.0286	0.0280	0.0285
D_1	0.0067	0.0071	0.0070	0.0071	0.0072	0.0072	0.0065	0.0067
D_2	0.0040	0.00386	0.00384	0.00385	0.00375	0.0040	0.0032	0.0051
F_{B111}/F_N	—	51.83	—	51.56†	52.39	51.64	—	51.42
D_3	—	0.0111	—	0.0111	0.0117	0.0111	—	0.0088
D_4	—	0.0185	—	0.0185	0.0169	0.0175	—	0.0191
(*c*) gold					Au5		Au V	
V/V_s	—	—	—	1.000	1.000		1.006*	
D	0.0722	—	0.0717	0.0720	0.0728		0.0720	
D_1	0.0309	0.0274	0.0306	0.0308	0.0313		0.0309	
D_2	0.0162	0.0164	—	0.0163	0.0161		0.0161	
F_{B111}/F_N	29.93	29.27	29.26	29.33†	29.32		30.04	

Notes. The entries at the left are the experimental values ('California' refers to Joseph *et al.* (1966) for copper, Joseph & Thorsen (1965) for silver, and Joseph *et al.* (1965) for gold); those on the right are the computed values. The 5 and 7 surfaces are designed to fit the 'chosen values' based on an assessment of the available data; the IV and V surfaces of Roaf were designed to fit the Shoenberg data, while his VI surfaces also took into account anomalous skin effect data.

The D are defined as follows: $D = (F_{B100} - F_{B111})/F_s$; $D_r = (F_{B100} - F_{Br})/F_s$, where r denotes the orientations at the following angles from ⟨100⟩:

	copper	silver	gold
1	16.0° in {110}	18.1° in {110}	22.0° in {110}
2	12.0° in {100}	13.4° in {100}	16.2° in {100}
3	27.0° in {100}	27.1° in {100}	—
4	—	43.0° in {110}	—

The entries marked † are taken from Jan & Templeton (1967) which were considered to be the most accurate results. However, the construction of Ag5 was made before these data were available and was based on a preliminary value, 52.35, derived by Joseph & Thorsen; this preliminary value was revised in Joseph & Thorsen's published paper. The entries marked * differ significantly from Roaf's published figures.

TABLE 6. VALUES OF COEFFICIENTS IN THE FERMI SURFACE REPRESENTATIONS

surface	C_0	C_{200}	C_{211}	C_{220}	C_{310}	C_{222}	C_{321}
Cu7	3.34901	0.19093	0.12668	−0.00799	−0.08531	−0.18798	−0.06261
Cu5	1.69167	0.00693	−0.42501	−0.01679	−0.03772	0	0
Cu5+	1.69096	0.00682	−0.42555	−0.01969	−0.03910	0	0
Cu5−	1.69237	0.00704	−0.42447	−0.01367	−0.03642	0	0
Ag7	0.62443	−0.03918	−0.60245	−0.08698	−0.08429	−0.00083	0.01406
Ag5	−0.89789	−0.12030	−0.90187	−0.14086	−0.09483	0	0
Ag5+	−0.88642	−0.11999	−0.90079	−0.14276	−0.09571	0	0
Ag5−	−0.90935	−0.12061	−0.90296	−0.13897	−0.09396	0	0
Au5	−2.26213	−0.16635	−1.25516	−0.09914	−0.12704	0	0
Au5+	−2.22160	−0.16486	−1.24673	−0.10341	−0.12756	0	0
Au5−	−2.30266	−0.16784	−1.26359	−0.09487	−0.12652	0	0

PHILOSOPHICAL TRANSACTIONS OF THE ROYAL SOCIETY A MATHEMATICAL, PHYSICAL & ENGINEERING SCIENCES

computed areas can be gauged from the very good agreement between the experimental and predicted dog's bone absolute areas since this feature was never used as a fitting parameter. Also included in this table are the computed 6-rosette and lemon areas (see p. 521) which agree within experimental error with available experimental data.

TABLE 7. ABSOLUTE VALUES OF F/F_s FOR SYMMETRY DIRECTIONS

	B100	B111	N	R	D	L	6R
copper							
Jan & Templeton (1967)	—	0.9502	0.03556	—	—	—	—
O'Sullivan & Schirber (1968)	0.9810	0.9509	0.03561	0.4027	0.4112	—	—
K. A. McEwen & J. Vanderkooy†	—	—	—	—	—	0.359	—
Cu7	0.9804	0.9498	0.03555	0.4022	0.4102	0.3592	1.8023
Cu5	0.9803	0.9497	0.03555	0.4021	0.4094	0.3598	1.8033
silver							
Jan & Templeton (1967)	—	0.9597	0.01861	—	—	—	—
M. J. G. Lee & K. A. McEwen†	—	—	—	—	—	—	1.808
Ag7	0.9899	0.9612	0.01862	0.4089	0.4205	—	1.8115
Ag5	0.9898	0.9613	0.01835	0.4088	0.4195	—	1.8125
gold							
Jan & Templeton (1967)	1.0094‡	0.9355	0.03190	0.4177‡	0.4037‡	—	—
Au5	1.0085	0.9357	0.03191	0.4157	0.4011	0.3571	1.8003

† These provisional figures were obtained in this laboratory in 1967.
‡ Jan & Templeton (personal communication).

Notes. The notation is as in table 2 and B100 and B111 refer to the central belly for the field along ⟨100⟩ and ⟨111⟩ respectively, L refers to the lemon orbit and 6R to the 6 cornered rosette.

Orientation dependence of F/F_s

Extensive computations have been made to determine how well the analytical surfaces reproduce the orientational dependence of frequency for the main orbits as determined in the present and earlier rotation experiments. The computed frequency variations are shown in tables 2 to 4 and are plotted in figures 2 to 4 together with the experimental data. It can be seen that the computed curves do agree very closely with the data even in ranges remote from those used in the fitting. A typical deviation between computed and experimental belly area differences in the {100} and {110} zones is 5×10^{-4}, which is comparable to the experimental error. The deviation is considerably worse in the {211} zone, but is probably not outside the much larger experimental error due to uncertainty in the precise orientation of the zone traversed.

Non-central belly areas

The subsidiary belly frequencies F_{B2} detected originally in silver by Joseph & Thorsen over certain regions of the {100} and {110} zones, are due to extremal areas of the Fermi surface whose centres lie a small distance above and below Γ. One of the most successful aspects of the new surfaces has been the accuracy with which they reproduce all the essential properties of these orbits although no features of the non-central area data have been used in the fitting. Programmes were written to compute belly area as a function of k_H away from Γ for arbitrary field angles in the {110} and {100} zones and typical results for (Cu7) are illustrated in figure 5. For small values of θ in the {110} zone the computed belly area decreases monotonically with k_H, but beyond

about $\theta = 16°$ the computed area begins to show a small lip and an extremal area, just before the orbit breaks up on the necks. For $\theta = 17°$, the non-central extremal area lies at 0.17 of the free electron radius k_s from Γ and the area difference $(F_{B1} - F_{B2})/F_s$ at $\theta = 17°$ is 0.0146 (cf. present experiment 0.0139; Joseph *et al.* 0.0141). As θ increases, the non-central extremum becomes more prominent until at $\theta = 23.0 \pm 0.5°$, d^2A/dk_H^2 becomes zero for a considerable distance around $k_H = 0$ and the two orbits merge (cf. present experiment 23.0°, Joseph *et al.* 23°. For $\theta \geqslant 23°$ and around $\theta = 54.74°$ ($\langle 111 \rangle$) the computed curves show only a central extremal area, in agreement with experiment. The ratio of central to non-central belly signal amplitudes is typically of the order of 5, which is about what would be expected from detailed consideration of the relevant curvature factors $\partial^2 A/\partial k_H^2$ and the cyclotron masses.

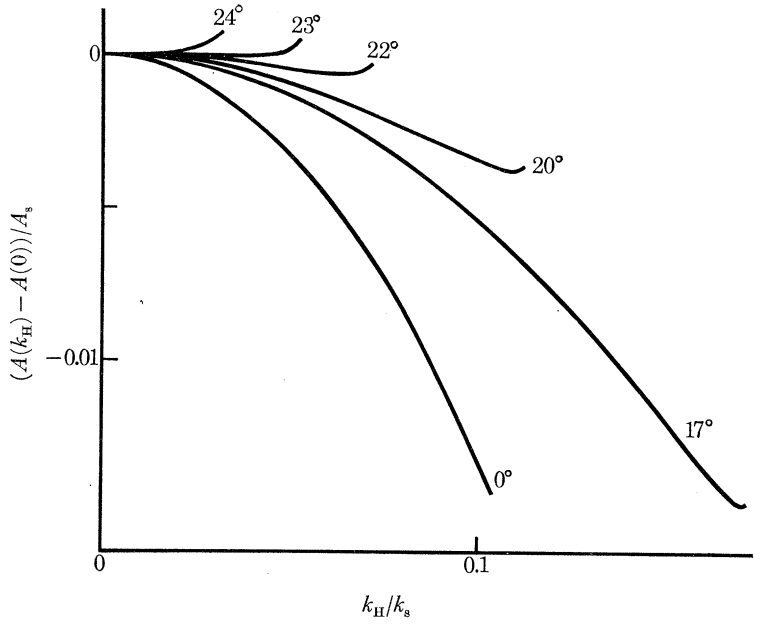

FIGURE 5. Belly areas A in copper as a function of k_H for various θ in a {110} zone computed from Cu7. The non-central minimum areas which occur near the end of the range of k_H for which an orbit exists and for angles between $\theta \simeq 16°$ and $\theta = 23°$ give rise to the subsidiary belly frequency F_{B2} whose angular variation is shown in figure 2.

As can be seen from figures 2 to 4 the computed area variations of F_{B2} in the {100} and {110} zones agree remarkably well with experiment (the agreement is comparable for the variations not illustrated). In agreement with experiment, only silver of the three noble metals has a Fermi surface with a non-central extremal area at and around $\langle 111 \rangle$ (for $\theta = 54.74°$, $k_H = 0.24k_s$); the computed area difference $(F_{B1} - F_{B2})/F_s$ at this orientation is 0.0121 (cf. Joseph & Thorsen 0.0115). It should be noted that at $\langle 111 \rangle$ in silver the central belly extremum is a maximum while it is a minimum in copper and gold; it is for this reason that the non-central minimum at $\langle 111 \rangle$ occurs only for silver.

Other non-central areas

Computations on the copper surfaces have revealed a lemon-shaped non-central extremal (minimum) area (figure 6) normal to $\langle 110 \rangle$ at $k_H = 0.86k_s$ with $F/F_s = 0.3598$ for Cu7 and 0.3592 for Cu5. Although the extremum is very sharp ($(d^2A/dk_z^2)^{-\frac{1}{2}} = 0.04$ as compared with 0.4 for a sphere) and the computed cyclotron mass (see p. 525) high (2.9 ± 0.3), oscillations of

appreciable amplitude from this orbit were obtained in a copper ⟨110⟩ crystal at 0.4 K and 9 T (90 kG) (K. A. McEwen & J. Vanderkooy, personal communication). The experimental value, $F/F_s = 0.359 \pm 0.002$, was in excellent agreement with prediction. This orbit should also be present in gold (with $F/F_s = 0.357$), but should be absent in silver (for both Ag5 and Ag7) as a consequence of the smaller neck size.

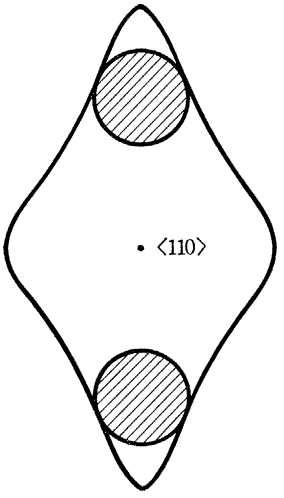

FIGURE 6. The lemon orbit in copper as computed from Cu7; it is normal to ⟨110⟩ and occurs at $\pm 0.86k_s$ from Γ, where the area is a minimum with respect to k_H.

Radius vectors

The radius vectors of Cu7, Ag7 and Au5 are given in tables 8*a*, *b* and *c*. The radii of Cu5 and Ag5 differ by only 0.15 % r.m.s. from the corresponding radii of the seven term expansions and the greatest difference in radius between Cu5 and Cu7 is only 0.3 % at ⟨100⟩. This suggests that the tabulated radii provide a reliable inversion of the area data, accurate to within say 0.2 %. The ⟨100⟩ and ⟨110⟩ radii k_{100}, k_{110} of Cu5 and Cu7 agree with the eleven-term cubic inversion scheme of Zornberg & Mueller (1966) to within their estimated accuracy of 1 %. (Zornberg & Mueller's calculations were based on the data of Joseph *et al.* (1966), i.e. very nearly the same data as used to compute Cu5 and Cu7.) To the same accuracy, k_{100} and k_{110} are in accord with the band structure calculations of Faulkner, Davis & Joy (1967), and with the direct experimental determinations of these two radii by Kamm (1966) using the magnetoacoustic effect. Recently, Lee (1969) has used the experimental frequencies F_{B100}, F_{B111} and F_N (which all agree well with those computed from Cu7) as input data for a phase shift analysis of the copper Fermi surface and finds agreement within about 0.1 % with the radii of Cu7 around both the {100} and {110} zones. Lee's analysis thus provides a specification of the Fermi surface which is as accurate as the Fourier expansion, but whose parameters (the phase shifts) are physically more meaningful. However the calculation of the surface in terms of this specification is more complicated than in terms of the Fourier expansion of equation (1).

Finally it should be mentioned that the necks of all the surfaces are circular to within computational error (less than 0.01 % in neck radius).

TABLE 8. RADIUS VECTORS OF THE FERMI SURFACES IN UNITS OF k_s

θ/deg \ ϕ/deg	0	5	10	15	20	25	30	35	40	45
					(*a*) Cu7					
0	1.0593	1.0593	1.0593	1.0593	1.0593	1.0593	1.0593	1.0593	1.0593	1.0593
5	1.0490	1.0490	1.0490	1.0490	1.0490	1.0490	1.0490	1.0490	1.0490	1.0490
10	1.0270	1.0271	1.0271	1.0271	1.0271	1.0272	1.0272	1.0272	1.0273	1.0273
15	1.0040	1.0041	1.0042	1.0044	1.0047	1.0050	1.0053	1.0055	1.0057	1.0057
20	0.9845	0.9846	0.9851	0.9858	0.9867	0.9877	0.9886	0.9894	0.9899	0.9900
25	0.9698	0.9701	0.9712	0.9728	0.9749	0.9771	0.9793	0.9811	0.9823	0.9827
30	0.9600	0.9606	0.9626	0.9656	0.9695	0.9739	0.9783	0.9820	0.9846	0.9855
35	0.9542	0.9553	0.9584	0.9634	0.9701	0.9778	0.9859	0.9931	0.9983	1.0001
40	0.9515	0.9530	0.9575	0.9649	0.9751	0.9877	1.0019	1.0160	1.0270	1.0313
45	0.9507	0.9526	0.9583	0.9679	0.9819	1.0007	1.0247	1.0544	1.0894	1.1173
50	0.9515	0.9536	0.9599	0.9709	0.9876	1.0117	1.0480	—	—	—
55	0.9542	0.9562	0.9622	0.9729	0.9896	1.0149	1.0559	—	—	—
60	0.9600	0.9614	0.9660	0.9745	0.9883	1.0091	1.0409	1.1072	—	—
65	0.9698	0.9703	0.9724	0.9771	0.9854	0.9986	1.0177	1.0432	1.0737	1.0935
70	0.9845	0.9837	0.9821	0.9814	0.9830	0.9879	0.9964	1.0072	1.0173	1.0217
75	1.0040	1.0014	0.9949	0.9877	0.9821	0.9794	0.9799	0.9826	0.9858	0.9872
80	1.0270	1.0218	1.0093	0.9950	0.9826	0.9737	0.9685	0.9664	0.9661	0.9662
85	1.0490	1.0406	1.0218	1.0014	0.9839	0.9707	0.9621	0.9572	0.9551	0.9545
90	1.0593	1.0490	1.0270	1.0040	0.9845	0.9698	0.9600	0.9542	0.9515	0.9507
					(*b*) Ag7					
0	1.0469	1.0469	1.0469	1.0469	1.0469	1.0469	1.0469	1.0469	1.0469	1.0469
5	1.0402	1.0402	1.0402	1.0402	1.0402	1.0402	1.0402	1.0402	1.0402	1.0402
10	1.0244	1.0244	1.0244	1.0244	1.0244	1.0244	1.0244	1.0244	1.0244	1.0244
15	1.0066	1.0066	1.0066	1·0067	1.0068	1.0069	1.0069	1.0070	1.0070	1.0070
20	0.9912	0.9912	0.9914	0.9917	0.9921	0.9925	0.9929	0.9932	0.9934	0.9935
25	0.9796	0.9798	0.9803	0.9812	0.9823	0.9835	0.9847	0.9856	0.9863	0.9865
30	0.9717	0.9722	0.9734	0.9753	0.9777	0.9804	0.9831	0.9854	0.9870	0.9876
35	0.9670	0.9677	0.9698	0.9732	0.9777	0.9829	0.9884	0.9932	0.9966	0.9978
40	0.9645	0.9655	0.9687	0.9739	0.9810	0.9899	0.9998	1.0093	1.0166	1.0194
45	0.9637	0.9651	0.9691	0.9759	0.9859	0.9991	1.0154	1.0338	1.0508	1.0585
50	0.9645	0.9659	0.9703	0.9781	0.9899	1.0067	1.0300	1.0638	—	—
55	0.9670	0.9682	0.9722	0.9796	0.9913	1.0088	1.0346	1.0793	—	—
60	0.9717	0.9725	0.9753	0.9807	0.9900	1.0045	1.0256	1.0564	—	—
65	0.9796	0.9796	0.9802	0.9825	0.9877	0.9968	1.0102	1.0271	1.0439	1.0519
70	0.9912	0.9901	0.9878	0.9859	0.9860	0.9893	0.9955	1.0034	1.0105	1.0134
75	1.0066	1.0041	0.9981	0.9913	0.9862	0.9839	0.9842	0.9863	0.9886	0.9896
80	1.0244	1.0202	1.0100	0.9982	0.9880	0.9809	0.9769	0.9751	0.9747	0.9746
85	1.0402	1.0343	1.0202	1.0041	0.9902	0.9798	0.9730	0.9689	0.9670	0.9664
90	1.0469	1.0402	1.0244	1.0066	0.9912	0.9796	0.9717	0.9670	0.9645	0.9637
					(*c*) Au5					
0	1.1306	1.1306	1.1306	1.1306	1.1306	1.1306	1.1306	1.1306	1.1306	1.1306
5	1.1055	1.1055	1.1055	1.1055	1.1055	1.1055	1.1055	1.1055	1.1056	1.1056
10	1.0597	1.0597	1.0598	1.0599	1.0600	1.0601	1.0603	1.0604	1.0604	1.0604
15	1.0190	1.0190	1.0193	1.0196	1.0201	1.0206	1.0210	1.0214	1.0216	1.0217
20	0.9884	0.9886	0.9892	0.9901	0.9912	0.9924	0.9935	0.9945	0.9951	0.9953
25	0.9674	0.9678	0.9690	0.9708	0.9731	0.9756	0.9780	0.9800	0.9814	0.9819
30	0.9542	0.9549	0.9570	0.9602	0.9644	0.9690	0.9736	0.9776	0.9802	0.9812
35	0.9468	0.9479	0.9512	0.9564	0.9633	0.9712	0.9795	0.9869	0.9922	0.9941
40	0.9434	0.9449	0.9495	0.9571	0.9675	0.9803	0.9946	1.0087	1.0196	1.0238
45	0.9424	0.9443	0.9501	0.9600	0.9742	0.9930	1.0167	1.0451	1.0757	1.0939
50	0.9434	0.9455	0.9519	0.9631	0.9799	1.0039	1.0389	1.1161	—	—
55	0.9468	0.9488	0.9548	0.9656	0.9823	1.0073	1.0465	—	—	—
60	0.9542	0.9556	0.9601	0.9684	0.9818	1.0021	1.0328	1.0885	—	—
65	0.9674	0.9677	0.9692	0.9729	0.9803	0.9926	1.0107	1.0349	1.0624	1.0783
70	0.9884	0.9869	0.9836	0.9805	0.9798	0.9829	0.9901	1.0000	1.0095	1.0136
75	1.0190	1.0145	1.0037	0.9913	0.9813	0.9754	0.9739	0.9755	0.9782	0.9794
80	1.0597	1.0500	1.0278	1.0038	0.9842	0.9706	0.9627	0.9592	0.9583	0.9582
85	1.1055	1.0871	1.0500	1.0146	0.9871	0.9681	0.9563	0.9499	0.9470	0.9463
90	1.1306	1.1055	1.0597	1.0190	0.9884	0.9674	0.9542	0.9468	0.9434	0.9424

Note. θ and ϕ are here the conventional polar angles with the pole at ⟨100⟩ and not to be confused with the θ and ϕ used elsewhere (to denote angles from ⟨100⟩ in the {110} and {100} zones).

PHILOSOPHICAL TRANSACTIONS OF THE ROYAL SOCIETY A MATHEMATICAL, PHYSICAL & ENGINEERING SCIENCES

Interpretation of cyclotron mass data

The area of an electron orbit on the constant energy surface $E(k) = E_F + \Delta E$ is larger than the area A of the corresponding orbit on the Fermi surface by an amount $(dA/dE)\,\Delta E$, proportional to the cyclotron mass of that orbit. Thus, if in addition to the shape of the Fermi surface, the cyclotron masses of several orbits are known, it should be possible to construct a neighbouring surface of constant energy and to use this surface to calculate the Fermi velocity at any point of the Fermi surface and the density of states, as well as the cyclotron masses of orbits not used in the fitting procedure. The Fermi velocity is proportional to $(\partial E/\partial k)_n$ and can therefore be obtained by computing the distance Δk along the normal between the two surfaces, since this distance is just $\Delta E/(\partial E/\partial k)_n$. The density of states and the electronic specific heat are proportional to $(\partial V/\partial E)$ and can therefore be computed from the difference ΔV in the volumes of the surfaces, and finally any cyclotron mass (even for a non-extremal area) can be computed from the difference ΔA in the appropriate areas of cross-section. The procedure for carrying out this program will be sufficiently illustrated by describing the calculations for copper; for silver and gold only a few essential details need be mentioned.

Construction of Cu5+ *and* Cu5−

To reduce the complexity of the computations, Cu5 rather than Cu7 was used to represent the Fermi surface and five cyclotron masses were chosen from the data of Koch, Stradling & Kip (1964) to cover a wide range of orientations and masses (see table 9). Cu5+ was then constructed so that the areas of each of the five orbits was increased by $0.006m$ (where m is the ratio of the cyclotron mass to the free electron mass m_0). The enlarged orbits are then the sections of a surface of energy $E_F + \Delta E$, where

$$\Delta E = \frac{0.006h^2}{2m_0 a^2}\left(\frac{3}{2\pi}\right)^{\frac{2}{3}}, \qquad (2)$$

ΔE is 43 meV for copper, and 34 meV for silver and gold. To provide some estimate of the errors involved in using a finite ΔE and to eliminate quadratic effects in ΔE by averaging, a similar surface Cu5− was also constructed in which the five areas were each *decreased* by $0.006\,m$. It can be seen from table 9 that the construction of Cu5± was successful in reproducing the five fitting masses within experimental error. As explained above, the surfaces Cu5± can be used to compute cyclotron masses for any field direction (and for any orbit) and as can be seen from figure 7 and table 9 they provide an interpolation between the five fitting points in very good agreement (typically within 0.02) with the data in the {110} zone. It can be concluded that, unlike the earlier data of Kip, Langenberg & Moore (1961) used by Roaf, the data of Koch *et al.* form a self-consistent set. Some of the masses computed from Cu5± are compared in table 9 with experimental data; the agreement between the computed and experimental estimates of the ⟨100⟩ limiting point mass and the ⟨110⟩ non-central extremal masses is especially noteworthy. The two masses taken from the data of Smith (1967) in the {211} zone are, however, not in good accord with computation. One of the applications of the + and − surfaces has been in the estimation of masses which have not yet been measured (for instance in order to calculate de Haas–van Alphen amplitudes), and included in table 9 are computed masses for the 6-rosette, lemon and some non-central belly orbits, the latter proving to be higher than the corresponding central belly mass as expected. The lemon and non-central belly masses were calculated using only Cu5 and Cu5− (these orbits unfortunately did not always exist on Cu5+ because of its larger neck size)

and are not as accurate as the other computed masses. In general where it was possible to calculate masses both from Cu5, Cu5 − and from Cu5, Cu5 +, the two estimates differed by no more than about 3 %, so the average mass (i.e. that from Cu5 ±) should successfully eliminate any errors arising from the use of a finite ΔE.

TABLE 9. CYCLOTRON MASSES IN COPPER, SILVER AND GOLD

	copper			silver			gold		
orbit	orientation (deg)	experiment	Cu5 ±	orientation (deg)	experiment	Ag5 ±	orientation (deg)	experiment	Au5 ±
B_1	$\theta = 0$	1.37 ± 01^1	1.371	$\theta = 0$	0.935 ± 005^5	0.938	$\theta = 0$	$\begin{cases} 1.19 \pm 03^6 \\ 1.08 \pm 03^7 \end{cases}$	1.133
B_1	$\theta = 18$	1.34 ± 01^1	1.345	$\phi = 30$	1.025 ± 01^5	1.024	$\theta = 20$	1.08 ± 03^7	1.081
B_1	$\theta = 54.7$	1.385 ± 01^1	1.381	$\theta = 54.7$	0.94 ± 01^5	0.940	$\theta = 54.7$	$\begin{cases} 1.09 \pm 10^6 \\ 1.14 \pm 03^7 \end{cases}$	1.089
N	$\theta = 54.7$	$\begin{cases} 0.46 \pm 02^1 \\ 0.46 \pm 02^2 \end{cases}$	0.461	$\theta = 54.7$	0.39 ± 01^3	0.390	$\theta = 54.7$	0.29 ± 01^4	0.289
D	$\theta = 90$	1.29 ± 01^1	1.292	$\theta = 90$	1.03 ± 01^5	1.031	$\theta = 90$	$\begin{cases} 1.00 \pm 10^6 \\ 1.00 \pm 03^7 \end{cases}$	1.002
B_1	$\theta = 70$	1.59 ± 02^1	1.585	$\theta = 17$	0.93 ± 01^5	0.925	$\phi = 25$	1.07 ± 10^4	1.10
B_1	$\phi = 30.1$	1.52 ± 08^2	1.54	$\theta = 25$	$\begin{cases} 0.98 \pm 01^5 \\ 1.06 \pm 03^3 \end{cases}$	0.98	—	—	—
B_1	$\psi = 7.3$	1.51 ± 02^8	1.425	$\theta = 45$	1.015 ± 01^5	1.005	—	—	—
B_1	$\psi = 35$	1.36 ± 02^8	1.505	$\theta = 62$	$\begin{cases} 0.96 \pm 01^5 \\ 0.95 \pm 05^3 \end{cases}$	0.96	—	—	—
B_1	$\psi = 58$	1.33 ± 02^8	1.54	$\theta = 70$	$\begin{cases} 1.03 \pm 01^5 \\ 1.02 \pm 03^3 \end{cases}$	1.035	—	—	—
B_1	—	—	—	$\phi = 20$	$\begin{cases} 0.945 \pm 01^5 \\ 0.92 \pm 03^3 \end{cases}$	0.935	—	—	—
D	$\phi = 41$	1.37 ± 07^2	1.32	$\phi = 40$	$\begin{cases} 1.09 \pm 01^5 \\ 1.15 \pm 03^3 \end{cases}$	1.10	—	—	—
R	$\phi = 2$	1.34 ± 07^2	1.32	$\phi = 0$	1.08 ± 01^5	1.08	$\phi = 0$	1.09 ± 07^6	1.02
N	$\theta = 30$	0.92 ± 02^1	0.975	$\theta = 36.9$	0.50 ± 02^3	0.515	$\theta = 29.9$	0.59 ± 02^4	0.605
N	$\theta = 80$	0.94 ± 02^1	0.945	$\theta = 72.5$	0.50 ± 02^3	0.515	$\theta = 79.6$	0.59 ± 02^4	0.56
lim	$\theta = 0$	0.48 ± 05^1	0.46	$\theta = 0$	0.42 ± 01^5	0.39	—	—	—
NC	$\theta = 90$	1.225 ± 005^1	1.225	$\theta = 90$	0.885 ± 005^5	0.865	$\theta = 90$	—	0.93
6R	$\theta = 54.7$	—	2.44	$\theta = 54.7$	—	1.93	$\theta = 54.7$	—	1.88
L	$\theta = 90$	—	2.9	—	—	—	$\theta = 90$	—	2.6
B_2	$\theta = 17$	—	1.51	$\theta = 25$	—	1.03	—	—	—
B_2	$\theta = 20$	—	1.475	$\theta = 50$	—	1.065	—	—	—
B_2	$\phi = 21$	—	1.67	$\theta = 54.7$	—	1.235	—	—	—
B_2	$\phi = 24$	—	1.60	$\theta = 62$	—	1.13	—	—	—

Notes. The notation describing orbits and orientations is the same as in table 2 with the following additions: 6R is the 6-rosette, L is the lemon, lim is the limiting point mass with H along ⟨100⟩ and NC is the extremal value of the mass as a function of k_H along ⟨110⟩ (this is the mass observed in cyclotron resonance and is quite different from the mass corresponding to the orbit of extremal area which is the lemon). All masses are expressed as ratios to the free electron mass. The experimental values are taken from (1) Koch *et al.* (1964), (2) Joseph *et al.* (1966), (3) Joseph & Thorsen (1965), (4) Joseph *et al.* (1965), (5) Howard (1965), (6) Shoenberg (1962), (7) Langenberg & Marcus (1964), (8) Smith (1967).

The first group of five entries shows the masses used as fitting parameters for determining the ± surfaces and the computed masses are therefore automatically in agreement with the experimental values to the extent that the fitting has been successful; for gold at $\theta = 0$ and 54.7° the mean of the two available experimental values was used as the fitting parameter. The second group of entries provides a test of the reliability of the ± surface by comparison of experimental and predicted values at other orientations and for other orbits; further computed masses for copper are shown in figure 7. For silver and gold the neck masses are given at the orientations for which spin splitting zeros occur ($gm = 1$) and the computed masses correspond to g values of about 1.94 ± 0.10 and 1.72 ± 0.10 respectively (the latter is the mean of the two values on either side of ⟨111⟩). The last group of entries are for masses which have not yet been determined experimentally.

PHILOSOPHICAL TRANSACTIONS OF THE ROYAL SOCIETY A MATHEMATICAL, PHYSICAL & ENGINEERING SCIENCES

Construction of Ag5+ *and* Ag5−

Four of the five silver masses chosen as fitting data (table 9) were taken from Howard (1965), but the fifth, the neck mass, was taken from Joseph & Thorsen (1965) whose estimate from the temperature dependence of de Haas–van Alphen amplitude seemed more reliable. (Their estimate of $m = 0.39 \pm 0.02$ has recently been confirmed by new cyclotron resonance experiments of Henningsen (1969) who found 0.37 ± 0.01.) The masses calculated from Ag5± are consistent to within about 0.015 with the rest of Howard's data in the {100} and {110} zones and this can be taken as the typical error of a general computed mass. The limiting point mass and the ⟨110⟩ non-central masses again agree well with experiment.

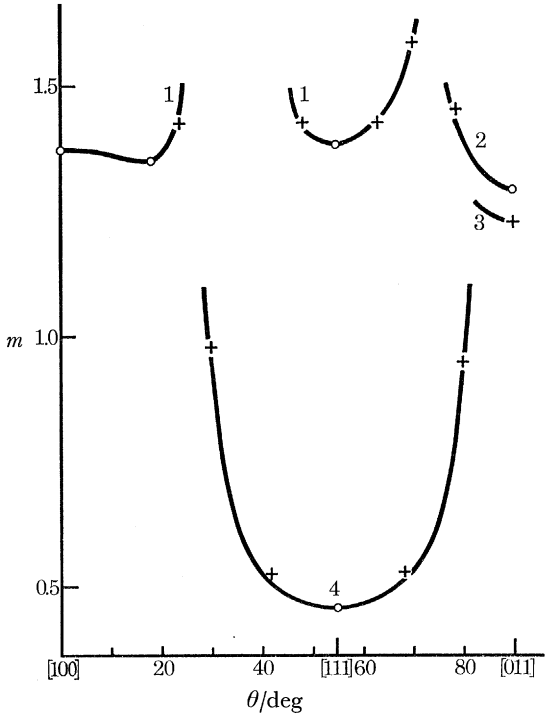

FIGURE 7. Orientation dependence of cyclotron mass in a {110} zone for copper; ——, experiment (Koch *et al.* 1964); ○, masses used as fitting data for Cu5±; +, additional masses calculated from Cu5±. The curves are (1) belly, (2) dog's bone, (3) ⟨110⟩ non-central mass, (4) neck.

Construction of Au5+ *and* Au5−

The information on cyclotron masses for gold is rather less comprehensive and accurate than for copper and silver. Thus the choice of five fitting masses was complicated by discrepancies between the various experimental estimates and the chosen values were compromises which may be in error by as much as 0.05 in m. As can be seen from table 9, the belly mass at ⟨111⟩ computed from Au5± could not be made to agree with its intended value, suggesting perhaps that the masses used do not quite form a self-consistent set. The masses computed from Au5± other than at the fitting orientations are probably reliable to ±0.05, though there is little additional information on gold belly cyclotron masses (other than the fitting ones) to substantiate this estimate of accuracy.

TABLE 10. FERMI VELOCITIES IN UNITS OF v_s

(*a*) Cu5±

θ/deg \ ϕ/deg	0	5	10	15	20	25	30	35	40	45
0	0.66	0.66	0.66	0.66	0.66	0.66	0.66	0.66	0.66	0.66
5	0.70	0.70	0.70	0.70	0.70	0.70	0.70	0.70	0.70	0.70
10	0.76	0.76	0.76	0.76	0.76	0.76	0.75	0.75	0.75	0.75
15	0.78	0.78	0.78	0.78	0.78	0.78	0.78	0.78	0.78	0.78
20	0.77	0.77	0.77	0.78	0.78	0.78	0.78	0.78	0.78	0.78
25	0.76	0.76	0.76	0.76	0.76	0.77	0.77	0.77	0.77	0.77
30	0.74	0.74	0.74	0.74	0.75	0.75	0.75	0.76	0.76	0.76
35	0.72	0.72	0.72	0.73	0.73	0.74	0.74	0.73	0.73	0.73
40	0.71	0.71	0.71	0.72	0.72	0.72	0.71	0.68	0.66	0.65
45	0.70	0.70	0.71	0.71	0.71	0.69	0.65	0.57	0.46	0.41
50	0.71	0.71	0.71	0.71	0.71	0.68	0.59	—	—	—
55	0.72	0.72	0.72	0.72	0.72	0.68	0.56	—	—	—
60	0.74	0.74	0.74	0.74	0.73	0.70	0.62	0.42	—	—
65	0.76	0.76	0.76	0.76	0.75	0.73	0.69	0.61	0.51	0.45
70	0.77	0.77	0.77	0.77	0.76	0.75	0.73	0.70	0.67	0.66
75	0.78	0.78	0.78	0.78	0.77	0.76	0.74	0.73	0.71	0.71
80	0.76	0.76	0.78	0.78	0.77	0.76	0.74	0.73	0.71	0.71
85	0.70	0.73	0.76	0.78	0.77	0.76	0.74	0.72	0.71	0.70
90	0.66	0.70	0.76	0.78	0.77	0.76	0.74	0.72	0.71	0.70

(*b*) Ag5±

0	0.97	0.97	0.97	0.97	0.97	0.97	0.97	0.97	0.97	0.97
5	1.01	1.01	1.01	1.01	1.01	1.01	1.01	1.01	1.01	1.01
10	1.07	1.07	1.07	1.07	1.07	1.07	1.07	1.07	1.07	1.07
15	1.11	1.11	1.11	1.11	1.11	1.11	1.11	1.11	1.11	1.11
20	1.11	1.12	1.12	1.12	1.12	1.12	1.12	1.12	1.13	1.13
25	1.10	1.10	1.10	1.11	1.11	1.11	1.12	1.12	1.12	1.12
30	1.09	1.09	1.09	1.09	1.10	1.10	1.10	1.10	1.10	1.09
35	1.07	1.07	1.07	1.07	1.07	1.07	1.06	1.05	1.04	1.04
40	1.06	1.06	1.06	1.06	1.05	1.03	1.01	0.97	0.93	0.92
45	1.05	1.05	1.05	1.05	1.03	0.99	0.92	0.82	0.70	0.65
50	1.06	1.06	1.06	1.05	1.02	0.96	0.84	0.60	—	—
55	1.07	1.07	1.07	1.06	1.03	0.96	0.81	0.50	—	—
60	1.09	1.09	1.09	1.08	1.05	1.00	0.88	0.66	—	—
65	1.10	1.10	1.10	1.10	1.08	1.05	0.97	0.87	0.75	0.69
70	1.11	1.11	1.12	1.12	1.11	1.08	1.04	0.99	0.95	0.93
75	1.11	1.12	1.12	1.13	1.12	1.11	1.08	1.05	1.03	1.02
80	1.07	1.09	1.11	1.12	1.12	1.11	1.09	1.07	1.05	1.05
85	1.01	1.04	1.08	1.11	1.12	1.11	1.09	1.07	1.06	1.05
90	0.97	1.01	1.07	1.11	1.11	1.10	1.09	1.07	1.06	1.05

(*c*) Au5±

0	0.80	0.80	0.80	0.80	0.80	0.80	0.80	0.80	0.80	0.80
5	0.95	0.95	0.95	0.95	0.95	0.95	0.95	0.95	0.95	0.95
10	1.04	1.04	1.04	1.04	1.04	1.04	1.04	1.04	1.04	1.04
15	1.01	1.01	1.01	1.01	1.01	1.02	1.02	1.02	1.02	1.02
20	0.96	0.96	0.97	0.97	0.97	0.98	0.98	0.98	0.98	0.98
25	0.92	0.92	0.92	0.93	0.94	0.95	0.95	0.96	0.96	0.96
30	0.89	0.89	0.90	0.91	0.92	0.93	0.94	0.95	0.96	0.96
35	0.87	0.87	0.88	0.89	0.91	0.93	0.94	0.95	0.96	0.96
40	0.85	0.85	0.87	0.89	0.91	0.93	0.94	0.94	0.93	0.92
45	0.85	0.85	0.86	0.89	0.91	0.93	0.91	0.85	0.73	0.67
50	0.85	0.86	0.87	0.89	0.92	0.92	0.86	0.62	—	—
55	0.87	0.87	0.89	0.91	0.93	0.93	0.85	—	—	—
60	0.89	0.89	0.90	0.92	0.94	0.95	0.89	0.69	—	—
65	0.92	0.92	0.93	0.94	0.95	0.96	0.94	0.89	0.79	0.72
70	0.96	0.96	0.96	0.96	0.96	0.96	0.95	0.94	0.92	0.91
75	1.01	1.01	1.00	0.98	0.96	0.95	0.94	0.93	0.92	0.92
80	1.04	1.04	1.02	1.00	0.96	0.93	0.91	0.90	0.89	0.88
85	0.95	1.01	1.04	1.01	0.96	0.92	0.89	0.87	0.86	0.86
90	0.80	0.95	1.04	1.01	0.96	0.92	0.89	0.87	0.85	0.85

Notes. θ and ϕ are, as in table 8, the conventional polar angles with the pole at ⟨100⟩. The values of v/v_s at the neck are 0.41, 0.35 and 0.62 for Cu, Ag, and Au respectively.

PHILOSOPHICAL TRANSACTIONS OF THE ROYAL SOCIETY A MATHEMATICAL, PHYSICAL & ENGINEERING SCIENCES

Orientation dependence of Fermi velocity

If at a general point (θ, ϕ), a normal is projected from the Fermi surface to intersect the corresponding $\pm$ surfaces, it follows from (2) that the intercept Δk between them is related to the Fermi velocity v at this point by

$$v/v_s = 0.006 k_s/\Delta k, \tag{3}$$

where v_s is the free electron sphere Fermi velocity and k_s is its radius. Computed velocities over a 5° grid for copper, silver and gold are given in tables 10*a*, *b* and *c*, and contours of the Fermi velocity for copper drawn from table 10*a* are shown in figure 8. The copper and silver Fermi velocities are probably reliable to $0.03v_s$ and most of this error is attributable to uncertainties in the cyclotron masses used to construct the $\pm$ surfaces; the ratio v_{100}/v_{110} in particular is a sensitive function of m_{B100}/m_{B111}. The velocities for gold are less accurate, probably only to $0.1v_s$, though improving to $0.02v_s$ in the neck region (where the accuracy should be just that of the neck cyclotron mass).

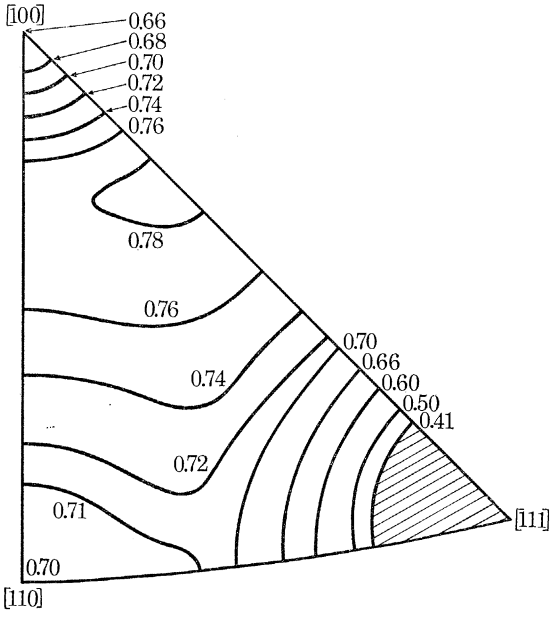

FIGURE 8. Contours of Fermi velocity (expressed as v/v_s) for copper, computed from Cu7.

Electronic specific heat

If ΔV is the difference in volume between the $\pm$ surfaces it is easily shown from (2) that the electronic specific heat coefficient γ is given by

$$\gamma = \frac{\Delta V/V_s}{0.018}\gamma_s, \tag{4}$$

where γ_s is the free electron specific heat coefficient given by

$$\gamma_s = \frac{\pi^2 R m_0 k a^2}{h^2}(\tfrac{2}{3}\pi)^{\frac{2}{3}}, \tag{5}$$

which is $5.00 \times 10^{-4}\,\mathrm{J\,mol^{-1}\,K^{-2}}$ for copper, 6.37 for silver and 6.36 for gold. The computed values of γ/γ_s (table 11) agree to within about 1 % with recent precision data of Martin (1968).

TABLE 11. ELECTRONIC SPECIFIC HEATS

metal	V/V_s 5 term surface	V/V_s 5+ surface	V/V_s 5− surface	γ/γ_s calc.	γ/γ_s expt.
copper	0.99956	1.01192	0.98672	1.400	1.384 ± 0.007
silver	0.99975	1.00906	0.99069	1.021	1.006 ± 0.006
gold	1.00024	1.01005	0.99038	1.093	1.087 ± 0.007

Notes. The calculated values are obtained from equations (4) and (5); the experimental values are those of Martin (1968). To avoid appreciable computational errors the volume had to be computed more accurately than was previously necessary; the accuracy achieved was of order 2×10^{-4} in V/V_s.

TABLE 12. SPIN SPLITTING ZEROS AND g VALUES FOR COPPER

orbit	orientation of zero/deg	gm	expt.†	Cu5±	g
B_1	$\theta = 23.6$ (23.8)	3	1.46	1.425	
B_1	$\theta = 48.1$ (48.3)	3	1.415	1.425	
B_1	$\theta = 63.4$ (63.3)	3	1.435	1.425	2.09 ± 0.02
B_1	$\phi = 27.2$ (27.0)	3	—	1.440	
B_1	$\psi = 7.3$	3	—	1.425	
D	$\theta = 78.8$	3	1.43	1.450	2.08 ± 0.02
D	$\phi = 36.5$ (36.8)	3	—	1.455	
N	$\theta = 41.6$ (41.7)	1	0.50	0.525	1.94 ± 0.05
N	$\theta = 68.2$ (68.1)	1	0.51	0.530	
R	$\theta = 6.7$ (6.8)	3	—	—	—
R	$\phi = 7.2$ (7.2)	3	—	—	—

† Koch *et al.* 1964.

Notes. The notation for orbits and orientations is as in table 2. The orientations at which zero amplitudes occur are those found in the present work followed by those given by Joseph *et al.* (1966) in brackets. The g values quoted are based on the averages of the m figures for each group.

Electronic g factors in copper

The field orientations at which certain de Haas–van Alphen amplitudes were observed to vanish because of vanishing of the spin-splitting factor $\cos(\pi gm/2)$ at $gm = 1, 3$, etc., are shown in table 12 and it can be seen that our estimates of these angles agree to within about 0.15° with those of Joseph *et al.* (1966). Values of g can be estimated if m is known at these orientations and slightly different estimates are obtained according as m is taken directly from interpolation or extrapolation of the data of Koch *et al.* or from the computed values based on Cu5± (also, of course, based on the data of Koch *et al.* but with a rather less direct interpolation); it may be noticed that the computed masses give slightly more consistent g values for belly orbits. The g values of about 2.09 ± 0.02 are considerably higher than the 2.031 ± 0.003 measured in the direct spin resonance experiment of Schultz & Latham (1965). Although spin resonance measures an average of g over the Fermi surface it is puzzling why this average should be so much less than the present de Haas–van Alphen estimate for belly orbits, which should be typical of most of the Fermi surface. This may perhaps indicate that many body effects are relevant.

The anomalous skin effect

Roaf constructed his six term surfaces Cu VI and Ag VI to be consistent within experimental error both with Shoenberg's de Haas–van Alphen data (upon which he based Cu IV and Ag IV) and with the anomalous skin effect measurements of Pippard (1957) and Morton (1960). To an accuracy of order 1 % in radius, the same Fermi surface was therefore able to account for two

widely differing electronic properties of a metal. Since the {110} dip D_1 of Ag VI is too large and the published properties of Cu VI contain computational errors (see notes to table 5), it was of interest to see how far the new surfaces Ag5, 7 and Cu5, 7, based only on the de Haas–van Alphen effect, were consistent with the anomalous skin effect and to what extent they improved upon Ag IV and Cu IV in this respect.

The orthogonal surface resistances R_x, R_y in the {110} zone were computed as fractions of the surface resistance R_s of a free electron sphere from the relation.

$$\frac{R_{x,y}}{R_s} = \left\{ \frac{2\pi k_s^2[(1/\epsilon+\epsilon)\tan^{-1}(1/\epsilon)-1]}{\int n_{x,y}^2 \, dS/(\cos^2\lambda+\epsilon^2)} \right\}^{\frac{1}{3}}, \tag{6}$$

where ϵ is the ineffectiveness angle, dS is an element of Fermi surface area, λ is the angle between the normal to the specimen surface and dS, n_y is the cosine of the angle between dS and the

TABLE 13. ANOMALOUS SKIN EFFECT

(*a*) copper

θ/deg ...	0	12	22	33	45.3	54.7	62	70.7	90
R_x/R_s									
Pippard (1957)	0.695	1.025	1.190	1.030	0.965	1.010	0.835	0.975	1.230
Cu7	0.715	1.085	1.145	1.075	0.950	1.040	0.800	1.005	1.270
Cu5	0.715	1.090	1.150	1.075	0.945	1.045	0.800	1.005	1.285
Cu IV	0.725	1.105	1.165	1.090	0.935	1.050	0.805	1.010	1.285
Cu VI	0.720	1.075	1.165	1.070	0.855	1.060	0.790	0.955	1.310
R_y/R_s									
Pippard (1957)	0.695	0.690	0.780	0.855	0.935	1.010	1.075	1.100	1.130
Cu7	0.715	0.740	0.790	0.820	0.895	1.040	1.050	1.140	1.195
Cu5	0.715	0.750	0.800	0.830	0.900	1.045	1.060	1.145	1.205
Cu IV	0.725	0.770	0.820	0.850	0.895	1.050	1.055	1.145	1.205
Cu VI	0.720	0.775	0.830	0.855	0.840	1.060	1.055	1.140	1.230

(*b*) silver

θ/deg ...	0	9	20	28	38	46	54.7	65	72	81	90
R_x/R_s											
Morton (1960)	0.860	0.990	1.100	1.085	1.060	0.990	1.000	0.850	1.080	1.115	1.085
Ag7	0.860	1.015	1.110	1.080	0.990	0.985	0.995	0.830	1.045	1.175	1.220
Ag5	0.845	1.015	1.120	1.085	0.980	0.980	1.010	0.815	1.040	1.180	1.235
Ag IV	0.825	1.020	1.125	1.090	0.980	0.980	1.005	0.805	1.045	1.190	1.225
Ag VI	0.900	0.990	1.060	1.085	1.030	1.005	0.940	0.885	1.070	1.135	1.125
R_y/R_s											
Morton (1960)	0.860	0.880	0.855	0.840	0.800	0.910	1.000	1.055	1.110	1.125	1.060
Ag7	0.860	0.840	0.790	0.760	0.785	0.885	0.995	1.070	1.125	1.155	1.165
Ag5	0.845	0.830	0.780	0.765	0.790	0.890	1.010	1.075	1.135	1.170	1.180
Ag IV	0.825	0.815	0.770	0.765	0.790	0.895	1.005	1.070	1.130	1.165	1.175
Ag VI	0.900	0.880	0.825	0.770	0.755	0.855	0.940	1.040	1.085	1.105	1.105

Notes. The experimental results of Pippard (1957) and Morton (1960) have been reduced to a fraction of the surface impedance of a free electron sphere by dividing by their best estimates of this quantity (which are 0.709 169.9 in their units respectively.) Pippard's results were also corrected for 5% polarization as described by Morton. The r.m.s. deviations of the computed values shown for Cu7, Cu5, Cu IV and Cu VI from the corresponding experimental values are 3.5, 3.8, 4.3 and 6.0%, and those of Ag7, Ag5, Ag IV and Ag VI from experiment are 5.0, 5.5, 5.5 and 3.8% respectively. Before calculating the r.m.s. figures, the experimental results were scaled by up to 2% where necessary to equate the means. Pippard's and Morton's surfaces P II and M remain the best fit to experiment (r.m.s. deviations 2.8 and 3.0%) but these surfaces do not predict correct de Haas–van Alphen frequencies.

PHILOSOPHICAL TRANSACTIONS OF THE ROYAL SOCIETY A MATHEMATICAL, PHYSICAL & ENGINEERING SCIENCES

common zone axis (y axis) of the {110} and {100} specimens, and n_x is the cosine of the angle between dS and the x axis (lying in the specimen surface perpendicular to y). Following Roaf, ϵ was taken as $1\frac{3}{4}°$ for both copper and silver; the answer does not depend critically on ϵ.

The present anomalous skin effect program was checked for any obvious errors by comparing our computed surface resistances for Roaf's Cu IV, Ag IV and Au V with those given in his table 2. The average and greatest deviations over 21 points between the two sets of figures were 1 and

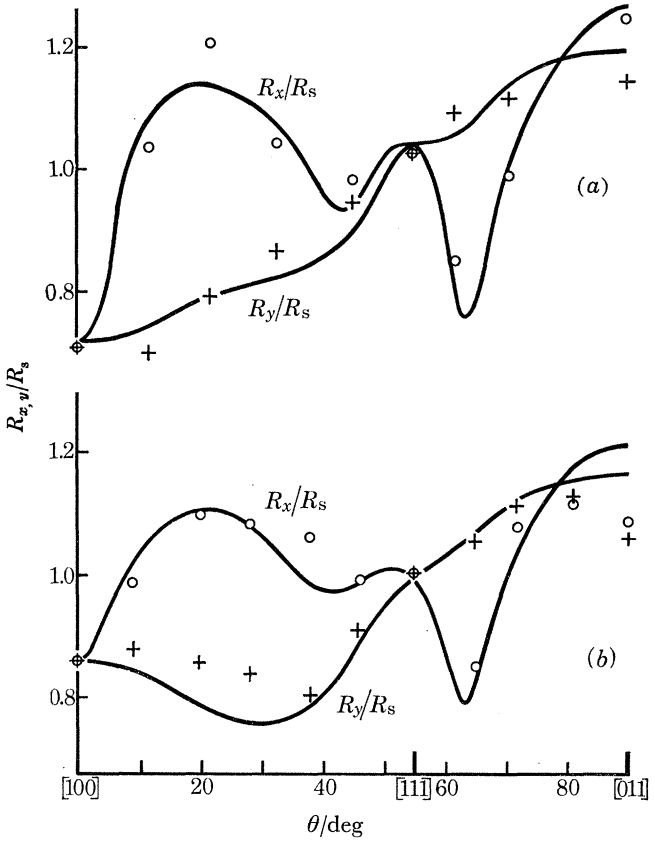

FIGURE 9. Anomalous skin effect surface resistance for (a) copper and (b) silver in a {110} zone; —— R_x/R_s, R_y/R_s computed from Cu7 and Ag7; the points ○ for R_x/R_s and + for R_y/R_s are experimental a, Pippard (1957); b, Morton (1960).

4 % respectively and arose from the different choice of step lengths in the two calculations. The present step lengths are thought to be fine enough to cause an error of no more than 2 %. Similar calculations on Cu VI and Ag VI however, revealed two 17 % and two 7% discrepancies respectively which could not be eliminated by reducing the step lengths, and which may perhaps be due to computing errors on Roaf's part.

The calculated surface resistances are compared with Pippard's and Morton's experimental results in figure 9 and table 13. It can be seen that the agreement is noticeably better for copper than for silver and that in copper the closest fit to experiment is provided by Cu7, for which the r.m.s. deviation between computed and experimental values is 3.5 %. In view of experimental and computational errors, each of about 2 %, this result can be regarded as satisfactory. The surfaces Cu5 and Cu IV give results very little different from those of Cu7, but Cu VI (which was intended to agree with the anomalous skin effect data as well as the area data) gives an appreciably worse fit (r.m.s. deviation 6 %).

For silver the various surfaces Ag IV, Ag5 and Ag7 (based solely on the de Haas–van Alphen data) again all give nearly identical results, with an r.m.s. deviation between computed and experimental points of about 5 %. This time, however, Roaf's Ag VI (tailored to take the anomalous skin effect data into account) does fit rather better (r.m.s. deviation 3.8 %). It can be seen that Ag7 departs particularly badly from Morton's results at ⟨110⟩ and although a 1 % improvement could be obtained here by increasing ϵ to 2.3° it is doubtful if any overall improvement would be obtained by changing ϵ.

The general semi-quantitative agreement so far revealed between the anomalous skin effect data and computations based on Fermi surfaces derived entirely from de Haas–van Alphen data is encouraging enough to suggest that the discrepancies may prove to be due to unsuspected errors in the data, or in the theory on which the calculations are based. Evidently it would be desirable to repeat and extend the anomalous skin effect measurements, but in the meantime there is no strong reason to doubt that the same Fermi surface can account for both the de Haas–van Alphen effect and the anomalous skin effect.

I should like to thank my supervisor Dr D. Shoenberg, F.R.S., most warmly both for his continued and lively interest in my work and for his considerable help in the preparation of this paper. My warmest thanks go also to Professor A. B. Pippard, F.R.S., for suggesting the rotation mechanism, to Dr D. J. Roaf for his invaluable help in explaining his computing procedures and to Dr I. M. Templeton for his generous gift of high quality copper crystals. I am also very grateful to Dr M. J. G. Lee, Mr K. A. McEwen and Dr J. Vanderkooy for undertaking experiments on the '6-rosette' and 'lemon' orbits, to Mr D. L. Randles for checking some of the computations and to Mr H. L. Davies, Mr F. T. Sadler and Mr P. Booth for their help with the apparatus and supply of liquid helium. Finally, I wish to thank the Science Research Council for a three-year maintenance grant.

References

Burdick, G. A. 1963 *Phys. Rev.* **129**, 138.
Faulkner, J. S., Davies, H. L. & Joy, H. W. 1967 *Phys. Rev.* **161**, 656.
Henningsen, J. O. 1969 *Phys. Stat. Sol.* (to be published).
Howard, D. G. 1965 *Phys. Rev.* **140**, 1705.
Jan, J-P. & Templeton, I. M. 1967 *Phys. Rev.* **161**, 556.
Joseph, A. S. & Thorsen, A. C. 1965 *Phys. Rev.* **138** A 1159.
Joseph, A. S., Thorsen, A. C. & Blum, F. A. 1965 *Phys. Rev.* **140**, A 2046.
Joseph, A. S., Thorsen, A. C. Gertner, E. & Valby, L. E. 1966 *Phys. Rev.* **148**, 569.
Kamm, G. N. 1966 *Bull. Am. phys. Soc.* **11**, 446.
Kip, A. F., Langenberg, D. N. & Moore, T. W. 1961 *Phys. Rev.* **124**, 359.
Koch, J. F., Stradling, R. A. & Kip, A. F. 1964 *Phys. Rev.* **133**, A 240.
Langenberg, D. N. & Marcus, S. M. 1964 *Phys. Rev.* **136** A 1383.
Lee, M. J. G. 1969 *Phys. Rev.* (to be published).
Martin, D. L. 1968 *Phys. Rev.* **170**, 650.
Morton, V. M. 1960 Ph.D. Thesis Cambridge University.
O'Sullivan, W. J. & Schirber, J. E. 1967 *Cryogenics* **7**, 118.
O'Sullivan, W. J. & Schirber, J. E. 1968 *Phys. Rev.* **170**, 667 (and addendum to be published).
Pippard, A. B. 1957 *Phil. Trans. Roy. Soc. Lond.* A **250**, 325.
Pippard, A. B. & Sadler, F. T. 1969 *J. scient. Instrum.* **2**, 101.
Roaf, D. J. 1962 *Phil. Trans. Roy. Soc. Lond.* A **255**, 135.
Schultz, S. & Latham, C. 1965 *Phys. Rev. Lett.* **15**, 148.
Segall, B. 1962 *Phys. Rev.* **125**, 109.
Shoenberg, D. 1962 *Phil. Trans. Roy. Soc. Lond.* A **255**, 85.
Shoenberg, D. 1968 *Canad. J. Phys.* **46**, 1915.
Shoenberg, D. & Stiles, P. J. 1964 *Proc. Roy. Soc. Lond.* A **281**, 62.
Smith, D. A. 1967 *Proc. Roy. Soc. Lond.* A **297**, 205.
Windmiller, L. R. & Ketterson, J. B. 1968 *Rev. scient. Instrum.* **39**, 1672.
Zornberg, E. I. & Mueller, F. M. 1966 *Phys. Rev.* **151**, 557.

PHILOSOPHICAL TRANSACTIONS OF THE ROYAL SOCIETY A MATHEMATICAL, PHYSICAL & ENGINEERING SCIENCES